www.ietdl.org

Published in IET Microwaves, Antennas & Propagation
Received on 10th June 2012
Revised on 31st December 2012
Accepted on 27th January 2013
doi: 10.1049/iet-map.2012.0326

ISSN 1751-8725

Ka-band waveguide rotary joint

Anatoliy Yevdokymov[1], Volodymyr Kryzhanovskiy[1], Vadim Pazynin[1], Kostyantyn Sirenko[2]

[1]Department of Mathematical Physics, Institute of Radiophysics and Electronics of National Academy of Sciences of Ukraine (IRE NASU), 12 Acad. Proskura str., Kharkiv, 61085, Ukraine
[2]Division of Computer, Electrical and Mathematical Sciences and Engineering, King Abdullah University of Science and Technology (KAUST), 4700 KAUST, Thuwal, 23955, Saudi Arabia
E-mail: yevdok@ire.kharkov.ua

Abstract: The authors present a design of a waveguide rotary joint operating in Ka-band with central frequency of 33 GHz, which also acts as an antenna mount. The main unit consists of two flanges with a clearance between them; one of the flanges has three circular choke grooves. Utilisation of three choke grooves allows larger operating clearance. Two prototypes of the rotary joint have been manufactured and experimentally studied. The observed loss is from 0.4 to 0.8 dB in 1.5 GHz band.

1 Introduction

Development of new and more efficient units of waveguide hardware has always been an important task in applied electrodynamics. A waveguide rotary joint is a classic and widely used unit of radar and antenna equipment [1–3]. Parameters of rotary joints directly affect the size and loss of antennas [1–5]. This paper presents the results of development of a rotary joint that acts not only as a waveguide junction between fixed transmission line and full-revolving antenna, but also serves as a support unit, which can carry antenna up to 2 kg in weight. The result of this arrangement is a significant reduction in weight and size of the rotating unit with waveguide elements. The measured electrodynamic parameters of the proposed joint satisfy generally accepted industry standards for such units [6–11].

The paper is organised in the following way: Section 2 discusses preliminary designs considerations; Section 3 presents numerical optimisation results; Section 4 details the final design of the rotary joint, its assemblage and tuning; and experimental studies of the joint are discussed in Section 5.

2 Design considerations

It is known that a rotary joint can be implemented on the basis of a circular waveguide with TE_{01}-, TM_{01}-, or TE_{11}-waves with circular polarisation [1–7]. Generators of TE_{01}-wave are usually large and technologically complex. Usage of TE_{11}-wave with circular polarisation results in the Doppler shift of emitted wave's frequency in case of rotating antenna and this is highly undesirable in modern coherent systems. Small-size designs of rotary joints generally use TM_{01}-wave, and we also selected this mode.

The proposed rotary joint consists of two circular waveguide segments. They are mounted with a clearance between them and are able to rotate about a common axis. Waveguide flanges are furnished with choke grooves which, under certain conditions and being finely tuned, reduce scattering loss and kill waves reflected from the circular waveguide discontinuity [2, 3, 12–14]. Thus, the first phase of development of the rotary joint is a correct choice of the clearance and choke settings for the required frequency band taking into account manufacturability and uncontrolled changes in the clearance during service. In our joint, we increase significantly the clearance between the rotating flanges using three choke grooves.

The scheme of the rotary joint is shown in Fig. 1. TM_{01}-wave propagates in the segment of circular waveguide 1. The second segment of circular waveguide 2 is installed with clearance a and is equipped with flat flange 3. Circular choke grooves 4 are located with period ℓ, and have depth h and width d. It is supposed that all the grooves are identical, and the planar waveguide, which is formed by the flanges outside of the grooves, supports only one radial propagating TEM-wave transverse electromagnetic wave, neither electric nor magnetic field in the direction of propagation that is absorbed by matched load 5. Owing to the axial symmetry, TM_{01}-wave is not transformed into low-order modes supported by the circular waveguide.

3 Numerical optimisation

The design of a rotary joint demands an accurate numerical modelling [4]. For numerical analysis of the structure an in-house software package was used. The core of the package, which ensures its accuracy and efficiency, is exact absorbing boundary conditions (EACs) implemented in finite-difference time-domain (FDTD) method [12, 15–17]. The relative error of the results presented in this paper does not exceed 0.1%.

The main goal of numerical optimisation is a finding of proper chokes' parameters. The simplified model of the junction, which is shown in Fig. 1, suits well for this goal.

© The Institution of Engineering and Technology 2013

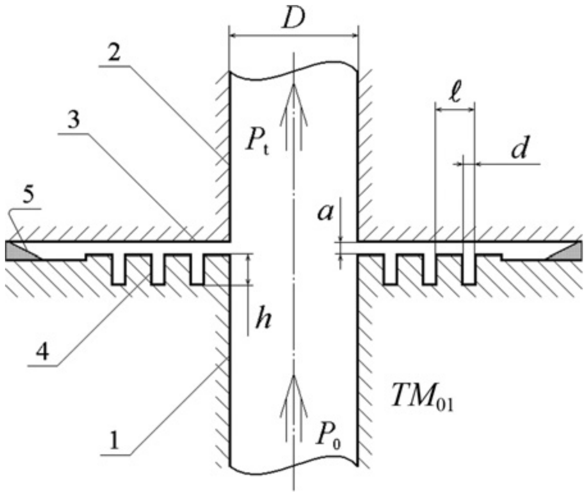

Fig. 1 *Scheme of the rotary joint*

The transitions from rectangular waveguides to circular waveguides are not included into the numerical model as: first, the transition is a ‘classic’ structure with known properties and operation principle [1]; and second, such inclusion will make the numerical model overcomplicated. We fine-tune these transitions experimentally before the final assemblage of the joint as detailed in Section 4.

Numerical optimisation results of the junction for the central frequency of 33 GHz are presented in Figs. 2–4. The dimensions of the grooves subject to their radial TEM-wave suppression purpose and ease of manufacture are chosen as: $d = 1$ mm, $h = 2$ mm, and $\ell = 2.8$ mm. The diameter of the circular waveguide is $D = 8$ mm. In numerical simulations, we assume that the junction is made of perfectly conducting metal, which is standard assumption in simulations of rotary joints [4, 5] and does not affect results in general [18].

The frequency dependence of the total loss in the junction is shown in Fig. 2. The parameter of the curves in Fig. 2 is a value of clearance a, which varies from 0.4 up to 1.2 mm with a step of 0.2 mm. Even in the worst-case of maximum clearance ($a = 1.2$ mm) the pass band is 3.1 GHz (from 31.3 to 34.4 GHz) with the insertion loss less than 0.05 dB

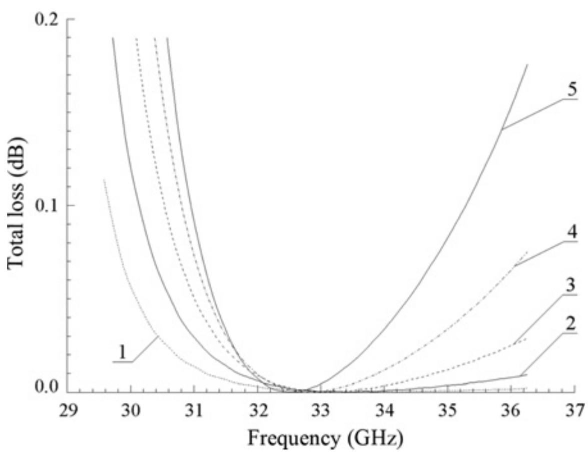

Fig. 2 *Numerically computed frequency dependence of total loss*

(1) $a = 0.4$ mm
(2) $a = 0.6$ mm
(3) $a = 0.8$ mm
(4) $a = 1.0$ mm
(5) $a = 1.2$ mm

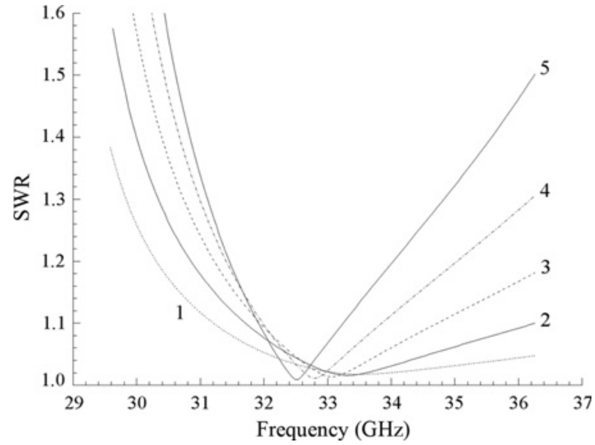

Fig. 3 *Numerically computed frequency dependence of SWR*

(1) $a = 0.4$ mm
(2) $a = 0.6$ mm
(3) $a = 0.8$ mm
(4) $a = 1.0$ mm
(5) $a = 1.2$ mm

(see curve 5 in Fig. 2). If the clearance is reduced to $a = 0.4$ mm, the operating frequency band is bounded only below by the value of $f_\ell = 30.1$ GHz (see curve 1 in Fig. 2).

The other important parameter of the waveguide unit is standing-wave ratio (SWR). The frequency dependence of SWR is shown in Fig. 3. Just like Fig. 2, the parameter of the curves in Fig. 3 is a value of clearance a. If we set ourselves the task of SWR value = 1.24, then the lower limit of the pass band is $f_\ell = 30.1$ GHz in the case of clearance $a = 0.4$ mm (curve 1, Fig. 3). In the worst-case of $a = 1.2$ mm, the pass band is from 31.3 to 34.4 GHz (curve 5, Fig. 3).

It should be noted that in a linear lossless two-port device, the value of SWR = 1.24 corresponds to a passed signal attenuation of 0.05 dB. Comparing the dependence of the loss with SWR (Figs. 2 and 3), we conclude that the loss in the system is caused mainly by a reflection loss of TM_{01}-wave from the slot in the waveguide. This conclusion is confirmed by the dependences shown in Fig. 4. γ is the ratio of field intensities in the adjacent grooves. Curve 1 is the ratio of the field intensity in the first (closest to the axis) and the second grooves, and curve 2 is the ratio of the field intensity in the second and the third grooves (the clearance

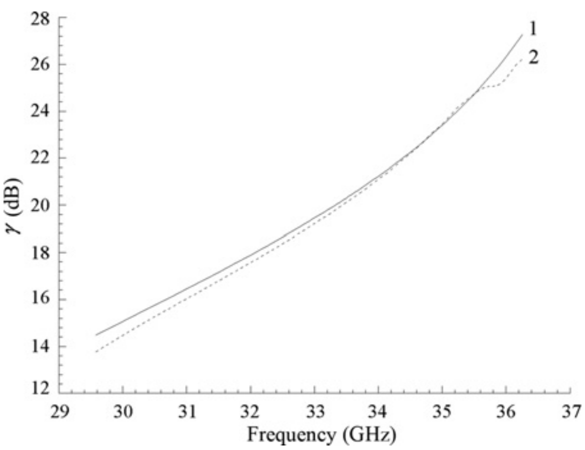

Fig. 4 *Ratio of field intensities in the adjacent grooves, a = 0.6 mm*

© The Institution of Engineering and Technology 2013

doi: 10.1049/iet-map.2012.0326

$a = 0.6$ mm). Both dependences are almost identical and we conclude that each of them shows the suppression of the outgoing TEM-wave between the flanges by one filter section. For example, for the frequency of 33.4 GHz the suppression by one groove is about 20 dB, and by the three-grooves filter (as in our case) it is about 60 dB. A recalculation of the absorbed power level in the load 5 (Fig. 1) into the insertion loss in the main track gives extremely small value of 5×10^{-5} dB, which can be neglected in our case. Thus, the aim to reduce scattering loss in the system of three grooves is attained.

Suppression of the wave passed through the system of the grooves by 50–60 dB may seem redundant at the first glance. However, this decision is justified by the fact that in real-world devices made in accordance with the scheme in Fig. 1, it is difficult to place high-quality absorber 5 in the clearance between the flanges. As a rule, in the absorber's place there are metal walls, gaskets and other elements that can form a cavity resonator with abruptly changing frequency response. As a result, there could be noticeable peaks and dips in the pass band of the rotary joint, which affect unfavourably the efficiency of the systems. Usage of three choke grooves makes it possible to get rid of the absorber in the clearance between the flanges and thereby reduce significantly the overall size of the device.

Selection of the clearance a should be based mostly on the acceptable SWR value. Two waveguide transitions from rectangular waveguide into circular one can be a source of reflected waves. Taking this fact into account, we conclude that the acceptable SWR value is 1.1. In the case of nominal clearance $a = 0.6$ mm and manufacturing accuracy of ± 0.2 mm, the maximum possible clearance is $a = 0.8$ mm. This provides the pass band of 2.75 GHz (from 31.95 to 34.7 GHz) or $\pm 4\%$ of the central frequency.

4 Design of the rotary joint

The simplified drawing of the rotary joint is shown in Fig. 5. Mount 1 supports turntable 3 via bearing 2. For simplicity of the drawing, the ring nuts that are intended for fixation of the bearing in its seat are omitted. Axial apertures and waveguide channels are made inside mount 1 and turntable 3. Diameter of the axial apertures is 8 mm, dimensions of the waveguide channels are 7.2 mm × 3.4 mm. Waveguide channels are closed by patch pieces 4 and 10 on the top and at the bottom. These patch pieces supplement turntable 3 and mount 1 with flanges of 24 mm × 24 mm. The TE_{01}-wave's field in the rectangular waveguide is matched (as detailed below) to the TM_{01}-wave's field in the circular waveguide using short-circuiting pistons 7 and 8, which are placed in the waveguide channels. Additional matching is provided by dielectric inserts 5 and 11 in the rectangular waveguide. Dielectric rings 6 and 9 are placed in the circular waveguide inside parts 1 and 3. These dielectric rings have built-in metal rings (outer diameter is 5 mm, and the section is 0.3 mm × 0.3 mm). Rings 6 and 9 act as modes filters and prevent excitation of TE_{11}-wave in the circular waveguide. Despite the fact that such filters suppress TE_{11}-wave only by a few decibels, utilisation of two rings eliminates completely the transmission coefficient's dependence on the angle between turntable 3 and mount 1. We need to use dielectric inserts 5 and 11 because residual SWR of the waveguide transition from rectangular waveguide into circular is 1.6. Inserts 5 and 11 compensate for the residual mismatch in the upper and lower transitions. Patch pieces 4 and 10 are equipped with screwed holes for fixing pistons 7 and 8.

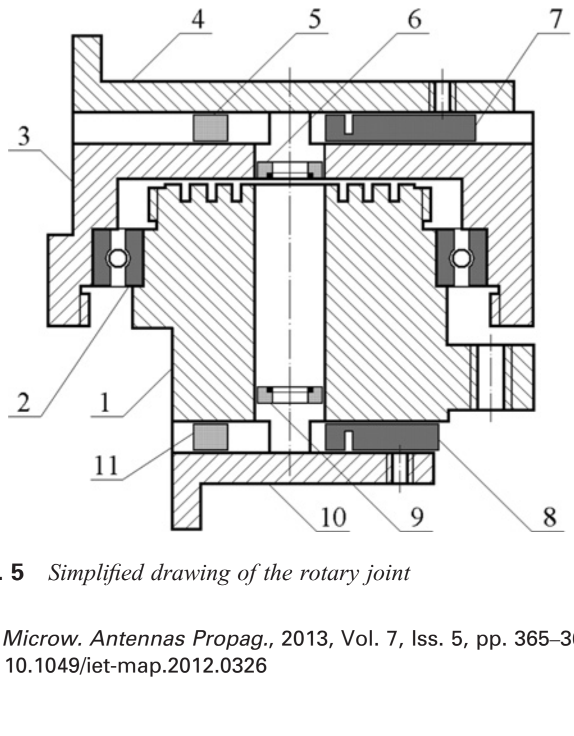

Fig. 5 *Simplified drawing of the rotary joint*

To assemble and tune the joint, the following steps are carried out:

1. Adjust thickness of dielectric inserts 5 and 11 to ensure SWR value of 1.6 in the rectangular waveguides on the working frequency. A dielectric insert with dimensions of 7.2 mm × 3.4 mm × 3.8 mm and relative permittivity 2.5 provides in a rectangular waveguide with dimensions 7.2 mm × 3.4 mm SWR value of 1.6. Small variations of the thickness may be needed if relative permittivity of a given insert differs from 2.5. To decrease SWR, the thickness should be reduced and vice versa.
2. Preassemble top and bottom parts of the joint. Top part: turntable 3 with installed ring 6, dielectric insert 5, piston 7 and patch piece 4. Bottom part: mount 1 with installed ring 9, dielectric insert 11, piston 8 and patch piece 10.
3. Tune preassembled top and bottom parts separately. Moving pistons 7 and 8, the SWR value not greater than 1.1 should be obtained within the band of at least ± 0.5 GHz of the working frequency. Fix pistons 7 and 8 after tuning.
4. Assemble the rotary joint connecting top and bottom parts. Check SWR value for the assembled joint, it should not exceed 1.4 on the working frequency. If needed, fine tune the joint moving pistons 7 and 8 slightly.

Appearance of the assembled rotary joint is shown in Fig. 6. Main parts are made of aluminium alloy. A protective coating of external surfaces and painting are allowed. Mount 1 and turntable 3 have additional round flanges for fastening an antenna on the turntable and the joint itself on a mounting surface. The rotary joint was designed keeping in mind the ease of manufacture, and, for example, soldering is excluded completely.

Owing to utilisation of the ball bearing with relatively large diameter, it is possible to use the rotary joint as a load-carrying swivel block for lightweight antennas. The structure was tested with 1 kg antenna (its aperture is 0.5 m). With fixed mount the allowable antenna weight is 2 kg.

© The Institution of Engineering and Technology 2013

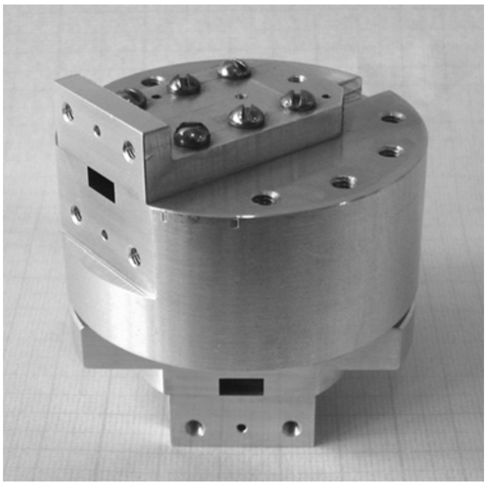

Fig. 6 *Photo of the prototype of the rotary joint*

5 Experimental study of the rotary joint

Two prototypes of the rotary joint were made with the circular waveguide diameters 8 and 8.2 mm. In both cases, the filter parameters (ℓ, d, h) were identical. The circular waveguide's diameter has an influence only on an alignment with the rectangular waveguides. Graphs of dependences of total loss and SWR on the frequency are shown in Figs. 7 and 8. Average loss in the pass band is from 0.4 to 0.8 dB. The specimen of the rotary joint with the circular waveguide's diameter of 8.2 mm has lower loss and slightly wider bandwidth of around 1.5 GHz. The operating frequency band does not exceed 1.5 GHz also, and is defined by acceptable SWR value of 1.4. All parameters of the rotary joint are highly stable with respect to the rotation angle between top and bottom parts of the joint. As the rotation angle changes between 0° and 360°, the deviations of the measured parameters do not exceed 2%; see Fig. 9 which plots measured total loss and SWR against the rotation angle for the prototype with the circular waveguide diameter 8 mm and the frequency 33 GHz. Moreover, this stability is preserved after 10 000 and 20 000 of full rotations with 2 kg load.

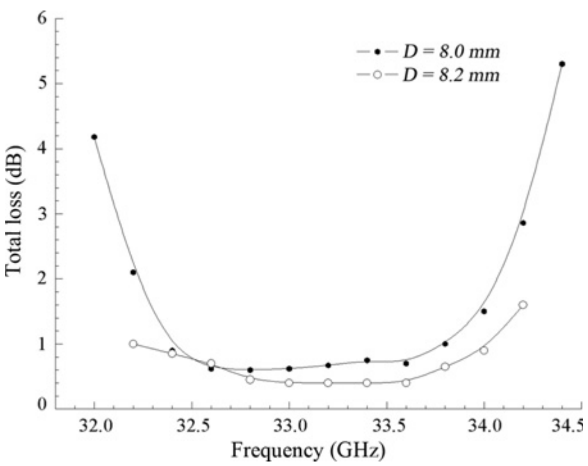

Fig. 7 *Experimentally measured frequency dependence of total loss*

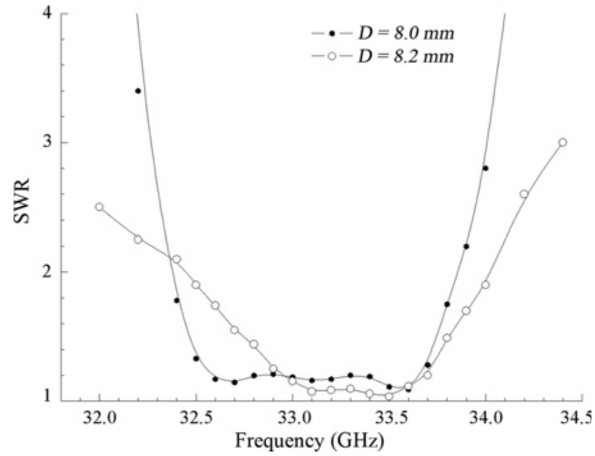

Fig. 8 *Experimentally measured frequency dependence of SWR*

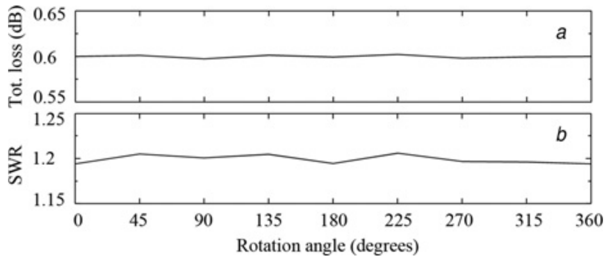

Fig. 9 *Experimentally measured dependences of*

a Total loss and
b SWR on the rotation angle, $D = 8$ mm, 33 GHz

Adjustment of the joint shows that the operating frequency band is defined mainly by a broadbandness of waveguide transitions between rectangular and circular waveguides. Known methods can be used to expand the operating frequency band as needed. They are: reduction of the rectangular waveguide's height [1], utilisation of waveguide tapers, and insertion of specific waveguide obstacles with given amplitude and phase characteristics. Nevertheless, our rotary joint excels these methods in manufacturability and is of a self-reliant interest.

6 Conclusions

The design of the rotary joint, which acts also as a support unit (mount) able to carry 2 kg antenna, is developed. It ensures the operating frequency band of 1.5 GHz with the central frequency of 33 GHz. The band-stop filter with moveable flanges was studied in details theoretically in order to increase the allowable clearance between the flanges. It was shown that in a rotary joint with a three-grooves filter the clearance between the flanges can be up to 0.6 ± 0.2 mm without utilisation of additional absorbers. Two prototypes of the rotary joint were built. Experimental data show very good coincidence with the numerically obtained.

7 References

1 Harvey, A.F.: 'Microwave engineering' (Academic Press, 1963)
2 Helszajn, J.: 'Passive and active microwave circuits' (Wiley, 1978)

© The Institution of Engineering and Technology 2013

doi: 10.1049/iet-map.2012.0326

3 Rizzi, P.A.: 'Microwave engineering: passive circuits' (Prentice-Hall, 1988)
4 McNamara, D.A., Hildebrand, L.T.: 'Fullwave analysis of non-contacting rotary joint choke sections using the generalised scattering matrix (GSM) approach', *IEE Proc. Microw. Antennas Propag.*, 2003, **150**, (1), pp. 5–10
5 Morini, A.: 'Design of a dual-band rotary joint operating in *X*- and *Ka*-bands', *IEEE Trans. Microw. Theory Tech.*, 2011, **59**, (6), pp. 1461–1467
6 de Mesquita, D.G., Bailey, A.G.: 'A symmetrically excited microwave rotary joint', *IEEE Trans. Microw. Theory Tech.*, 1970, **18**, (9), pp. 654–656
7 Chang, T.H., Yu, B.R.: 'High-power millimeter-wave rotary joint', *Rev. Sci. Instrum.*, 2009, **80**, (3), pp. 034701–034701-4
8 http://antennasystems.com/product/waveguide-single-joint/28WRJU.html, accessed January 2013
9 http://www.fairviewmicrowave.com/pdfParts/SR1803A.PDF, accessed January 2013
10 http://www.millitech.com/pdfs/specsheets/IS000086-WRJ.pdf, accessed January 2013
11 http://www.advancedmicrowave.com/rotary-joint-wg.html, accessed January 2013
12 Pazynin, V.L., Sirenko, K.Y.: 'The strong approach to analysis of transients in the axially symmetrical waveguide units', *Telecommun. Radio Eng.*, 2006, **65**, (1), pp. 1–18
13 Sirenko, K.Y.: 'Slot resonances in axially symmetric radiators of pulse-modulated and monochromatic TM-modes', *Telecommun. Radio Eng.*, 2007, **66**, (1), pp. 9–21
14 Chernobrovkin R.E., Ivanchenko I.V., Korolev A.M., Popenko N.A., Sirenko K.Y.: 'The novel microwave stop-band filter' i. *Active and Passive Electronic Components*, 2008, **2008**, ID745368
15 Sirenko, K., Pazynin, V., Sirenko, Y., Bagci, H.: 'An FFT-accelerated FDTD scheme with exact absorbing conditions for characterizing axially symmetric resonant structures', *Prog. Electromagn. Res.*, 2011, **111**, pp. 331–364
16 Sirenko, K.Y., Sirenko, Y.K.: 'Exact absorbing conditions in the initial boundary-value problems in the theory of open waveguide resonators', *Comput. Math. Math. Phys.*, 2005, **45**, pp. 490–506
17 Sirenko, Y.K., Strom, S., Yashina, N.P.: 'Modeling and analysis of transient processes in open resonant structures. New methods and techniques' (Springer, 2007)
18 Sirenko, K., Pazynin, V., Sirenko, Y., Bagci, H.: 'Compression and radiation of high-power short RF pulses. I. Energy accumulation in direct-flow waveguide compressors', *Prog. Electromagn. Res.*, 2011, **116**, pp. 239–270

doi: 10.1049/iet-map.2012.0326
© The Institution of Engineering and Technology 2013